Implementation of Error Correction on IBM Quantum Computing Devices

Sangat Sharma, Suresh Basnet and Raju Khanal

Journal of Nepal Physical Society
Volume 8, No 1, 2022
(Special Issue: ICFP 2022)
ISSN: 2392-473X (Print), 2738-9537 (Online)

JNPS, **8** (1), 7-15 (2022)
DOI: http://doi.org/10.3126/jnphyssoc.v8i1.48278

Published by: Nepal Physical Society
P.O. Box: 2934
Tri-Chandra Campus
Kathmandu, Nepal
Email: nps.editor@gmail.com

ICFP 2022
ISSN:2392-473X (Print)
2738-9537 (Online)

Research Article ©Nepal Physical Society
DOI: http://doi.org/10.3126/jnphyssoc.v8i1.48278

Implementation of Error Correction on IBM Quantum Computing Devices

Sangat Sharma,[1, a)] Suresh Basnet,[1, 2, b)] and Raju Khanal[1, c)]

[1)] *Central Department of Physics, Tribhuvan University, Kathmandu, Nepal*
[2)] *Department of Physics, GoldenGate International College, Tribhuvan University, Battisputali, Kathmandu, Nepal*

[a)] *Corresponding author:sangatsharma766@gmail.com*
[b)] *Electronic mail: sbplasma1986@gmail.com*
[c)] *Electronic mail: plasmanepal@hotmail.com*

Abstract. Quantum noise cannot be avoided in the quantum computing devices due to unstable nature of qubits and signals. The error caused by quantum noise can be detected and corrected using different error correcting codes. In this work, we have tested the feasibility and accuracy of three qubit bit flip and phase flip error correcting code in quantum computer provided by International Business Machine Quantum Experience (IBM QX) cloud platform. Among five quantum processors, ibmq_ourense is found to have highest average accuracy $77.9\% \pm 3.09\%$ on all qubits simultaneously. Three qubit**s** bit flip error correction circuit gave correct output $89.9\% \pm 1.01\%$ of the time on average. Similarly three qubits phase flip error correction circuit give $88.05\% \pm 1.89\%$. The measurement error mitigation has improved the accuracy of bit flip and phase flip error correction code by 5.01% and 7.01% respectively on average. The error rate shows that the error in quantum computations are random in nature and can be corrected. IBM QX quantum computer are suitable for only small scale quantum computation and demonstrate purpose. Furthermore, the accuracy of error correction codes can be increased with the use of higher accuracy quantum qubits and quantum gates.

Keywords: Bit-flip error, phase-flip error, quantum circuit, quantum gates, qubits

Received:3 March 2022; **Revised**:4 April 2022; **Accepted**:28 April 2022

INTRODUCTION

Computer has important role in physics to understand and realize different natural phenomena and these computers are simulating many classical problems efficiently; however, they are not capable of simulating the quantum mechanical problems efficiently. The quantum computing and quantum information processing is necessary for efficient simulation of different natural phenomena in the subatomic level [1]. Other uses of quantum computers are quantum key distribution, more robust encryption technology and quantum data storing devices [2]. The quantum computer uses qubit as its fundamental component. The ability of qubit to remain on superposition state is the key strength of qubit over classical bit. Speed and accuracy of quantum computer is directly related to efficiency of creating and manipulating coherent superposition of quantum states [3, 4]. In fact the fundamental physical component that differentiate the quantum computer from classical one is quantum bit (qubit) [5]. A qubit is the mathematical entity that carries quantum information and it is also known as physical object which carry quantum information. The qubit is a quantum analogous of classical bit 0 and 1. The classical bit can exist either on state 0 or 1, but the qubit can exist in continuum states between $|0\rangle$ and $|1\rangle$, until observed. During the observation or measurement state of qubit is destroyed to classical bit either 0 or 1 [2]. The conventional quantum states that describes the single qubit computational basis states are:

$$|0\rangle = \begin{pmatrix}1\\0\end{pmatrix} \quad \text{and} \quad |1\rangle = \begin{pmatrix}0\\1\end{pmatrix} \tag{1}$$

The state of an arbitrary qubit is given by $|\psi\rangle = \alpha|0\rangle + \beta|1\rangle$, where α and β are the complex number associated with probability amplitude of the qubits. To apply the different quantum mechanical operators on the state of qubit, quantum gates are used. The most used gates in quantum computation are: quantum NOT (X) gate, CNOT (CX) gate and Hadamard (H) gate, where X and H gates are single qubit gates and CNOT gate is multiple qubits gate, which has one control qubit and one target qubit [2]. The quantum not gate flips the spin of qubit which is analogous to classical NOT gate, whereas the Hadamard gate keeps the qubit in superposition state which is fundamental property of qubit. The effect of different gates on the qubit of state $|\psi\rangle = \alpha|0\rangle + \beta|1\rangle$ are;

$$\text{Pauli-X:}\ \ \alpha|0\rangle + \beta|1\rangle \longrightarrow \beta|0\rangle + \alpha|1\rangle \tag{2}$$

$$\text{Hadamard:}\ \ \alpha|0\rangle + \beta|1\rangle \longrightarrow \alpha\frac{|0\rangle + |1\rangle}{\sqrt{2}} + \beta\frac{|0\rangle - |1\rangle}{\sqrt{2}} \tag{3}$$

and

$$\text{Pauli-Z:}\ \ \alpha|0\rangle + \beta|1\rangle \longrightarrow \alpha|0\rangle - \beta|1\rangle \tag{4}$$

Quantum gates are arranged in a net like structure called quantum circuit and this is widely used model for quantum coding. The quantum information is passed to quantum circuit in the form of qubits and are manipulated through gates and measured at the end of operation. The circuit is read from left to right. Classical components are also added for reliable storing of information, the quantum circuit is different from classical circuit in many ways: the lines in quantum circuit are not actual wires as in the classical circuit and denote axis of time. The operation given in circuit are performed in specific order (left to right) [6]. Several operations of classical circuit are not available for quantum circuit such as feedback, fan-in, fan-out etc. The measurement is an interesting operation in quantum circuit where it collapses the state of a qubit $\alpha|0\rangle + \beta|1\rangle$ to classical bit 0 and 1 with probability $|\alpha|^2$ and $|\beta|^2$, respectively. These qubits are very sensitive to noise and other signals used to control quantum computer [7]. The sustainable coherence of superposition of quantum information is challenging task in field of quantum computing. This process requires far more precise and better maintenance of quantum system [8, 9] than currently available. The noise introduced by any cause, relaxation and decoherence corrupts the quantum state of qubit [9]. This effect of noise must be eliminated to perform large scale quantum computation and to maintain the correct state of quantum information through out the computation. The general framework of reducing or eliminating the effect of noise on quantum computation and quantum information processing is called quantum error correction [8].

In the recent years, the quantum error correction has gained considerable interest due to successful development of quantum computation theories and small scale real quantum computers [9, 10, 11]. As the realization of quantum computer increases, the necessity of error correction increases more rapidly. Hence, several error correcting codes are also developed and systematically studied in past few years [11, 12, 13, 14, 15]. Stabilizer code [5], three qubit error correcting code, the Shor code, surface code [16] are some examples of quantum error correcting codes. This codes are found suitable for large scale quantum computation on superconducting circuit [17], trapped ions [18] and diamond valency centers [19]. Recently, even the silicon spin qubits are considered promising for large scale quantum computation with the help of surface code and increasing 2 qubit gate fidelity to 99.5% [20]. With the advancement of cloud computing, the International Business Machine (IBM) released a cloud of quantum computing platform, IBM Quantum Experience (IBM QX) and it is available for public too. That provided the opportunity of running quantum computer (up to 20 qubit) over cloud. Some remarkable works are also done in this cloud platforms. Quantum artificial life [21], Quantum router circuit for quantum computer [22], experimental study on violation of mermin inequality using 5 qubit quantum computer [23] are some remarkable works are also done in this cloud platforms. The state of bit can be copied easily and measurement does not affect the state of classical bit, but in case of quantum mechanical error correction, following problem occurs [9]:

i) Information of quantum bit cannot be copied easily i.e., it is impossible to construct unitary operator U_c that performs following operation to qubit $|\psi\rangle$,

$$U_c(|\psi\rangle \otimes |0\rangle) \rightarrow |\psi\rangle \otimes |\psi\rangle \tag{5}$$

ii) Qubit can suffer from bit-flip as well as phase-flip error in contrast to only one bit flip error in classical bit.

iii) Measurement of wave function of qubit as the part of error correction collapses quantum information.

Normally errors occurring on quantum computation are bit flip error and phase flip error in which the bit-flip error is most dominant error in quantum computation. Suppose we have a qubit on state $\alpha|0\rangle + \beta|1\rangle$, then effect of bit flip is [2]:

$$\alpha|0\rangle + \beta|1\rangle \rightarrow \beta|0\rangle + \alpha|1\rangle \tag{6}$$

On the other hand, the phase flip error is also a dominant in quantum computation and it has no analog error in classical computer. The phase flip error changes sign of complex number associated with vector $|1\rangle$ in computational basis. The effect of phase flip error is [2]:

$$\alpha|0\rangle + \beta|1\rangle \rightarrow \alpha|0\rangle - \beta|1\rangle \tag{7}$$

In this work, we have ran a small scale quantum algorithms and perform experiments over cloud and studied the implementation of simple 3-qubit error correcting code in IBM QX. The obtained results revealed that the numbers of quantum gates used in the quantum circuit causes error on qubits and gates as well. On quantum circuits, three qubits bit flip and phase flip error correction can be employed with an error of less than 20%. The mistake, however, was not found in the same circuit as the simulator. The accuracy has increased by 7.01 percent as a result of the measurement error minimization. Furthermore, with higher-accuracy quantum qubits and quantum gates, the results of error correction may approach those of the simulator.

METHODOLOGY

Any quantum error correction algorithm consists three steps: encoding, decoding and correcting errors. Encoding section entangles data qubit to other qubits and prepares syndrome qubits. Decoding is process of finding qubit(s) in which error is introduced and another step is correcting error qubits by suitable gate operations [11]. We repeat these steps for bit-flip error and phase-flip error corrections. In addition, we examine the evolution of error in quantum bits with the increase in number of gate operations. We have qubit in the pure state which is written as [2]:

$$|\psi\rangle = \alpha|0\rangle + \beta|1\rangle \tag{8}$$

This information has encoded and transmitted through a noisy quantum channel and receiver receives the information in encoded state with noise and examines the syndrome bits with the application of data qubit correction. The error in qubit may be either bit flip type or phase flip type. For the bit flip error correction, simply X gate is applied to final state of qubit. This is quantum analogous of classic error correcting code and it can correct the bit-flip error in only one qubit. In classical error correcting codes, data qubit is simply copied for the multiple times, but no-cloning theorem forbids to make an exact copy of quantum state i.e., $|\psi\rangle \rightarrow |\psi\rangle|\psi\rangle|\psi\rangle$ is forbidden [6]. Instead we prepare extra two qubits on state $|0\rangle$ and make an entanglement of three qubits which are independently sent through quantum channel. The circuit diagram of bit flip correcting code is depicted in Fig. 1. The CNOT gates are used to make entanglement of data qubit. Since the initial state of syndrome qubit is known as receiver can track the error by measuring syndrome qubit.
The initial data state is $\psi = \alpha|0\rangle + \beta|0\rangle$ with $(\alpha = 0, \beta = 1), (\alpha = 1, \beta = 0)$, and $(\alpha = \beta = 1/\sqrt{2})$ where α, and β are the complex number and $|\alpha|^2 + |\beta|^2 = 1$. The bit flip error is introduced manually on each qubit one at a time and encoder section entangles all qubits with the data qubit (q_2). The error is introduced corresponds to the qubits on the error section, while the decoder section removes the error on data qubit (if any) and flips the state of syndrome bit. The Taffoli gate is required on both encoder and decoder sections as the Taffoli gate changes the target qubit if and only if both the control qubits are on state $|1\rangle$. The measurement of qubits destroys the state of qubit to either 0 or 1 classical bit. The value of α and β is measured by simulating circuit for many times and using normalizing condition and this measured state is stored on classical register. The quantum and classical bits are mapped logically to diagnose the error with more precision. In present case, the syndrome qubits are mapped to most significant classical bits and data qubit to the least significant classical bit.
Suppose we encode the state $\alpha|0\rangle + \beta|1\rangle$ using bit-flip error correcting circuit into 3 qubits as $\alpha|000\rangle + \beta|111\rangle$. Formally, the encoding can be written as;

$$|0\rangle \longrightarrow |0_L\rangle \equiv |000\rangle \quad \text{and} \quad |1\rangle \longrightarrow |1_L\rangle \equiv |111\rangle \tag{9}$$

where $|0_L\rangle$ and $|1_L\rangle$ denote the states are logical $|0\rangle$ and logical $|1\rangle$ not physical $|0\rangle$ and physical $|1\rangle$. After making the entanglement, we now send same information through three qubits independently. Due to very basic nature of quantum error circuit, some assumptions should be made such as:

i) Probability of error must be less than $1/2$. For three qubits circuit, error should not be in two or more qubits simultaneously.

ii) Only a bit flip error can be corrected by circuit at a time. In case of other errors, results become worse.

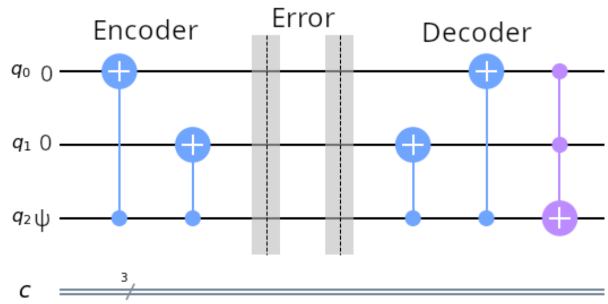

FIGURE 1. Schematic diagram of bit-flip error correcting circuit for three qubits.

The encoded quantum states may be changed due to the quantum noise which can be found by syndrome bit measurement, gives four possible outcomes. For error on syndrome qubits, nothing is done because information is protected on data qubit. However, when error is on data qubit, it is fixed by applying Taffoli gate. If the error is occurred on data qubit, Taffoli gate applies bit flip again and original state is recovered. The efficiency of any quantum circuit is measured by a quantity called fidelity, which measures how far the two states are. The fidelity (ρ) between a pure state $|\psi\rangle$ and arbitrary state ρ is given by [2]:

$$\rho = [(1-p)^3 + 3p(1-p)^2]|\psi\rangle\langle\psi| + \ldots.. \tag{10}$$

where p is the probability of error on quantum channel. The variation of minimum fidelity as the function of

probability with and without error correction is depicted in Fig. 2, which clearly shows that the error correction code works only for the probability $p < 1/2$.
If the error in quantum computation is phase flip type, Hadamard gates are used at the end of encoding and beginning of decoding section for each qubit [24]. The Hadamard gate changes basis of qubit from $|0\rangle, |1\rangle$ to $|+\rangle, |-\rangle$ and written as

$$|+\rangle \equiv (|0\rangle + |1\rangle)/\sqrt{2} \text{ and } |-\rangle \equiv (|0\rangle - |1\rangle)/\sqrt{2} \quad (11)$$

The circuit diagram for the phase flip error is shown in Fig. 3. We have performed the error correction for different state as in bit flip code. The Hadamard gates have been applied before and after quantum channel and error correction for the different state has been performed. First Hadamard gate changes computational basis (Z-basis) to (+) basis. The phase flip error introduced on (+) basis is changed to bit-flip error and detected using same method as before. Again, the Hadamard gate is applied after quantum channel to reverse the changes made by previous Hadamard gate. Three qubits are prepared on the state $|0\rangle$. On data qubit, control NOT gate is applied to make it on state $|1\rangle$ while other qubits are left unchanged. The encoder circuit entangles data qubit with other qubits. The Hadamard gates are applied on all qubits that changes the basis of operation to (+). The phase flip error is manually introduced on one of the qubits at a time and again the Hadamard gates are applied on all the qubits, and basis is restored to computational state (Z-basis).

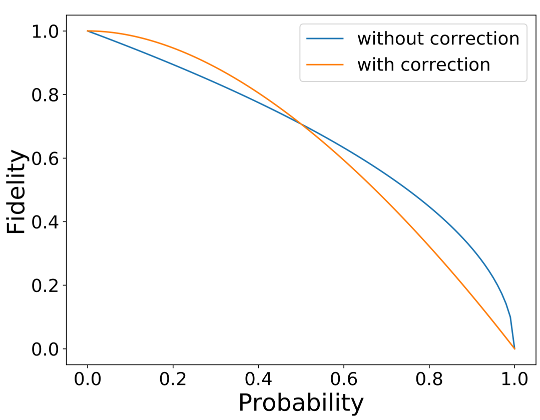

FIGURE 2. Fidelity of three qubits error correcting code.

There may be some background noise which may present during qubit preparation and measurement and such noises can be mitigated using simple algebraic noise mitigation technique. Different qubit states are simply prepared without any other operation and measured. The three qubits measurement can give have eight different possible states: 000, 001, 010, 011, 100, 101, 110 and 111. If each of eight states are prepared and measured for 1000 times, maximum counts are obtained for the prepared state but other seven state also may arise as noise and a 8x8 calibration matrix (M) is obtain. If C_N is the count matrix obtained by measuring output of any error correcting experiment, the measurement of error mitigated counts can be obtained as [25];

$$C_M = M^{-1} \times C_N \quad (12)$$

where M is the 8×8 calibration matrix.

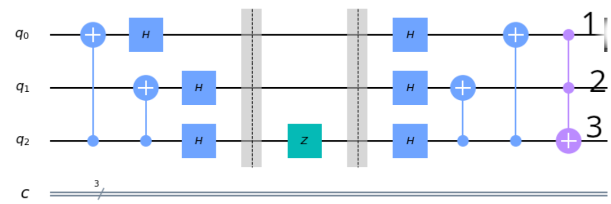

FIGURE 3. Circuit diagram of phase flip error correction.

RESULTS AND DISCUSSIONS

IBM has provided several computational back-ends for public with various architecture and computing power. The accuracy of available back-end is calculated by counting number of times the correct state obtained. A best back-end is selected by computing accuracy of each on different test circuits. This process is repeated for different circuits, identical to our circuits on error correction on all available back-ends. The variation of an accuracy percentage of 1000 measurements for different test back-ends is shown in Fig. 4. The mean accuracy is taken after several computations on different test circuits and error bar shows the standard error of mean accuracy. The circuit is assumed to be accurate if all the qubit states match their theoretical state. It is found that an accuracy of individual qubit is usually higher than this value. The ibmq_ourense and ibmq_vigo have higher accuracy on almost all circuit and ibmq_burlington has low accuracy. Despite of the same circuit and similar back-end architecture, there is variation on the error rates and this variation is due to the variation of error on individual qubit and error on different gate operations on different back-ends. On average ibmq_ourense has 77.9±3.09 percent accuracy as highest accuracy among five back-ends and the waiting time on ibmq_ourense is lower than others, so we have used this back-end for error correction purpose. A back-end have different qubits and each qubits have different error rate. For the efficient computation, we have to map our circuit to ibmq_ourense such that overall error is minimized. It is usually done automatically by IBM QX and sometimes it needs to be reconfigured. Three qubits error correcting code works only when probability of error is small ($p < 0.5$). Thus, we have studied evolution of error on different qubits by increasing number of operations on qubits. With the increase in number of gate operation, error rate also increased but rate of increment on individual qubit is found to be different. This shows the fundamental difference in the nature of qubits and their error rate.

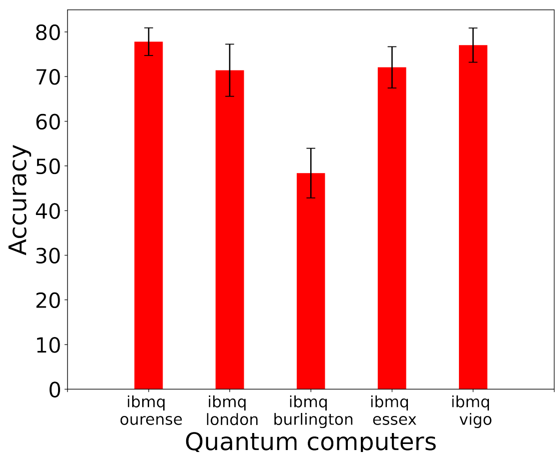

FIGURE 4. Bar graph showing accuracy of different back-ends on test circuits.

For the bit flip error correction, circuit is prepared as shown in Fig. 1 with error on third qubit. When the data qubit was on state $\psi = \alpha|0\rangle + \beta|1\rangle$ with $\alpha = 1$ and $\beta = 0$, the probabilities of different state are obtained as shown in Fig. 5. The histogram shows difference in probabilities of different states for ibmq quantum computer and the local simulator with bit flip error. Local simulator is qasm_simulator provided on Qiskit API which acts as an ideal quantum computer and ibmq_ourense which is noisy quantum computer. The local simulator does not show any error on measurement, but ibmq_ourense shows error. The ibmq_ourense has finished the work with 90.9% accuracy on data qubit, 89.4% on first qubit and 94.0% accuracy on second qubit. The simple circuit shows error about 10% due to the error on qubit and gate itself. If the qubits and gates are made more robust, quantum computer result approaches simulator result.

Number of counts of different states when error is manually applied to q_0, q_1 and q_2 for data qubit state $|1\rangle$ and superposition state are presented in Tables I and II. The resultant outcomes of the computation with errors on different qubits are kept on corresponding rows of the tables. The column label on each table denotes the final states of three qubit when measured. All eight possible classical states are obtained with small proportion. The maximum number of counts for data qubit state $|1\rangle$ have third classical bit 1 as shown in Table I. In Table II, there are around 50% counts for state 0 and same for state 1 which shows the data qubit is in superposition state before measurement. In 2^{nd} and 3^{rd} row, when error is introduced in q_0 and q_1, the dominant state is found to be other than 111. This shows that one of the qubit is flipped, but the state of data qubit is same as initial state. The decoder section corrects the error on data qubit and gives state same as initial.

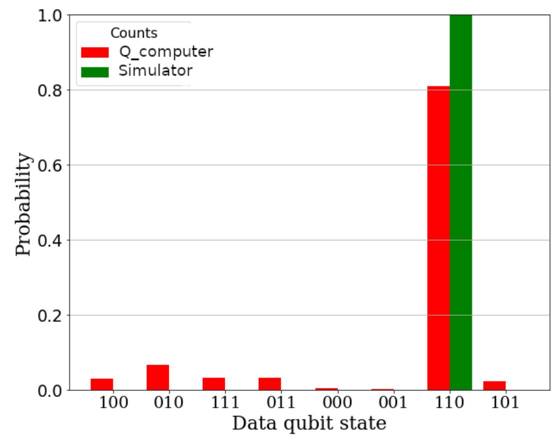

FIGURE 5. Result of measurement error correction circuit for data state.

TABLE I. Number of counts for 1000 shots with initial data qubit at state $|1\rangle$.

Error	000	001	010	011	100	101	110	111
None	68	804	16	40	11	37	13	11
1	24	57	60	796	6	7	29	21
2	14	100	9	4	67	767	26	13
3	127	20	49	35	47	53	69	710

TABLE II. Number of counts for 1000 shots with initial data qubit at superposition state.

Error	000	001	010	011	100	101	110	111
None	428	434	30	31	26	24	15	12
1	48	35	397	413	16	20	35	36
2	43	41	19	16	460	336	30	55
3	11	10	56	39	45	23	380	436

Fig. 6 shows error rates in different qubits for different states (a) state $|0\rangle$ and (b) state $|1\rangle$ with the error in q_0, q_1 and q_2. The error is introduced in any one of the qubit one at a time. The average error is least in all state when no manual error is introduced. We couldn't find significant variation of error rates on the qubits. There is no pattern on error and error is found to be random. The randomness in measurement occurs due to quantum decoherence, physical noise and cannot be controlled remotely. This shows that the error is random and error correcting circuit performed well on any condition of bit flip error with overall error less than 20%. Fig. 6(a) shows that the average error is relatively high in qubit q_0 while in Fig. 6(b), the average error is high in qubit q_2. This result shows data qubit state is protected in all cases with error less than 18%. The error rate in data qubit has not a definite pattern that shows the error is independent of qubit in which error is introduced.

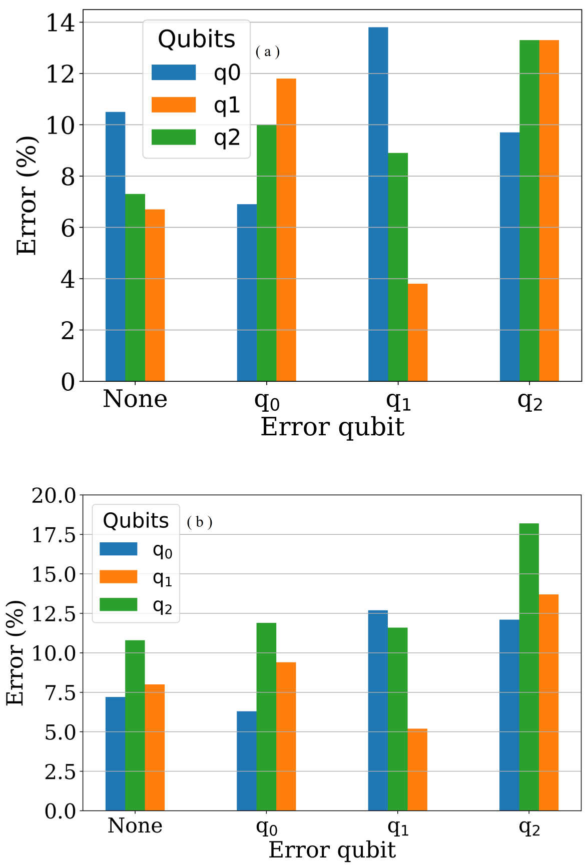

FIGURE 6. Error rate for data qubit for $|0\rangle$ and $|1\rangle$ state (a) state $|0\rangle$ and (b) state $|1\rangle$.

Phase flip error correction circuit is slight modified form of bit flip error correction circuit as shown in Fig. 3. The data qubit is prepared for three different states $|0\rangle$, $|1\rangle$ and superposition state. Tables III, IV and V show the result of measurements of three qubits for data qubits on (a) state $|0\rangle$, (b) state $|1\rangle$ and (c) superposition state. The error qubit is specified by row heading on each table and first column shows error qubit and other eight columns are result of measurement of the corresponding states. First two bits of each state represent binary equivalent of error qubit and last bit denotes data bit which needs to be protected against any errors on the circuit. In Table III, a large number of counts occurs for the state with least significant bit (last bit) 0 and other states also exist with small proportion indicating errors. Similarly, in Table IV, most occurred state is the state with last bit 1.

TABLE III. Result of phase-flip error correction for state $|0\rangle$

Error	000	001	010	011	100	101	110	111
None	722	88	46	35	43	16	16	34
q_0	55	18	825	33	2	1	0	25
q_1	96	22	10	7	777	40	30	18
q_2	17	21	52	50	41	29	748	42

TABLE IV. Result of phase-flip error correction for state $|1\rangle$.

Error	000	001	010	011	100	101	110	111
None	201	506	48	47	42	76	49	31
q_0	12	51	66	775	15	16	31	34
q_1	15	93	27	23	46	716	41	39
q_2	32	24	95	33	38	70	55	653

TABLE V. Result of phase-flip error correction for the superposition state.

Error	000	001	010	011	100	101	110	111
None	362	501	30	25	32	29	11	10
q_0	65	40	444	361	18	16	28	28
q_1	35	57	17	13	371	449	32	26
q_2	18	17	35	37	41	62	432	358

In Table V, most occurred states are on nearly 50-50 ratio. This concludes the preservation of data qubit state even with error is occurred and with no manual error present on the circuit; however, some error is obtained in each state. Thus, there is some noise and other errors are presented. The last row of each table is related to data qubit while the first row of each table is output of error correction circuit without any error. The first two bits of most probable state for first row are 00 indicating no error at all. On the second row, the most probable state has 01 as its first two bits. This indicates that the error is on first qubit. On the third row, the error bits have state 10 indicating error on qubit q_1. On the last row, the error qubit have state 11 indicating error on q_2. For the error on q_0 and q_1, the error qubit is successfully identified. Since error on the syndrome bit does not affect the data qubit, only error occurred indication is performed.

In case of error on the data qubit, state is recovered and error indication is also done to obtain initial state of the data qubit.

For overall acceptance of the given circuit for phase flip error correction, error in the individual qubit is to be calculated. Figure 7 shows accuracy of individual qubit on each state of computation performed. The error qubits are separated by the different colors and the data qubit states are separated by columns. An accuracy of individual qubit for all experiments are calculated and average is taken for each error state. An accuracy is almost same for all the state and qubits and the maximum accuracy is for qubit q_0 on the state $|0\rangle$ with 90.5%±1.66%, whereas the minimum accuracy is for the qubit q_0 on the state $|1\rangle$ (79.7% ± 5%)). The superposition state has highest accuracy (on average) with low deviation. This result shows phase flip error correcting circuit can be implemented on ibmq_ourense.

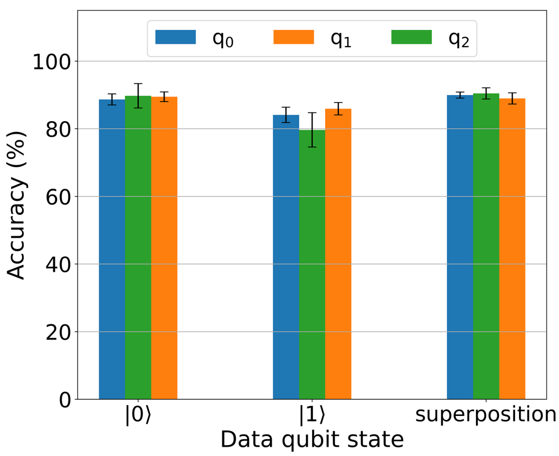

FIGURE 7. Accuracy of qubits on the different states.

One of the type of errors that can be addressed without physical access to quantum computer is the measurement error. A calibration matrix is calculated for all the possible states with three qubits. This matrix gives the correction factor in order to obtain more correct result and the calibration matrix is obtained as:

$$\begin{bmatrix} 0.951 & 0.038 & 0.038 & 0.001 & 0.030 & 0.000 & 0.001 & 0.000 \\ 0.016 & 0.936 & 0.002 & 0.042 & 0.001 & 0.029 & 0.001 & 0.000 \\ 0.020 & 0.001 & 0.937 & 0.040 & 0.000 & 0.011 & 0.029 & 0.001 \\ 0.001 & 0.016 & 0.015 & 0.909 & 0.000 & 0.001 & 0.001 & 0.038 \\ 0.012 & 0.000 & 0.000 & 0.000 & 0.946 & 0.034 & 0.048 & 0.001 \\ 0.000 & 0.009 & 0.000 & 0.000 & 0.009 & 0.899 & 0.000 & 0.034 \\ 0.000 & 0.000 & 0.008 & 0.000 & 0.014 & 0.001 & 0.905 & 0.023 \\ 0.000 & 0.000 & 0.000 & 0.008 & 0.000 & 0.250 & 0.015 & 0.903 \end{bmatrix}$$

The principal diagonal elements show the correct result percentage for the given state from 000 to 111 and off diagonal elements on each row represent error occurred for correct state given by diagonal element. When we operate this matrix with the result, we have obtained more accurate results. The error mitigation is performed for all the states and error on all qubits. Figure 8 shows the comparative counts of noisy, mitigated and simulator results. Figure 8(a) shows the result of operations for the data qubit on state $|0\rangle$ with error on the third qubit for the bit flip error and the simulator gives 100% corrected results. It is clearly seen that there is improvement in probability of correct state after applying measurement error mitigation technique and probability of incorrect is decreased after applying error mitigation. Figure 8(b) shows the result of similar operation with data qubit on the state $|0\rangle$ and with data qubit on superposition state, respectively. The simulator result is 100% in agreement with theory for all the measurements. Figure 8(c) shows the comparison of probability of different states for noisy, mitigated and simulator counts when state of data qubit is in the $\frac{1}{\sqrt{2}}|0\rangle + \frac{1}{\sqrt{2}}|1\rangle$ state. Hence, the probability is nearly 0.5 for both the classical states 110 and 111. These clearly indicate the error mitigation improves probability of true states. By applying the error mitigation technique, the obtained results have been improved by an amount 5.2% in terms of magnitude. Also, the error improvement ratio is nearly same for all the measurements. This shows that the measurement error occurs while probing quantum state of qubit and doesn't depend upon initial state of qubit as well.

Figure 9 shows the comparative probabilities of different data qubits state before and after the application of measurement error mitigation on the phase flip error correction circuit. The average probability of different data qubits state is shown and it is found that the improvement on probability of each state is nearly same which is 0.071 in average.

CONCLUSION

With the help of Qiskit API in python, we have performed the three qubits bit flip error correction and phase flip error correction experiment on IBM QX. We test a sample circuit on different quantum computers in IBM QX, in spite of their similar qubit architecture, ibmq_ourense is found to be more accurate and stable with accuracy 77.9%±3.09% for our work. The error rate on each qubit of same quantum chip is found to be different and increases linearly with number of quantum gates used. This restricts use of large and complex circuit implementation on IBM QX with current hardware and three qubits error correction code seems suitable for implementation on the ibmq_ourense for demonstration purpose. For three qubits bit flip error correcting code, the state $\frac{1}{\sqrt{2}}(|0\rangle + |1\rangle)$

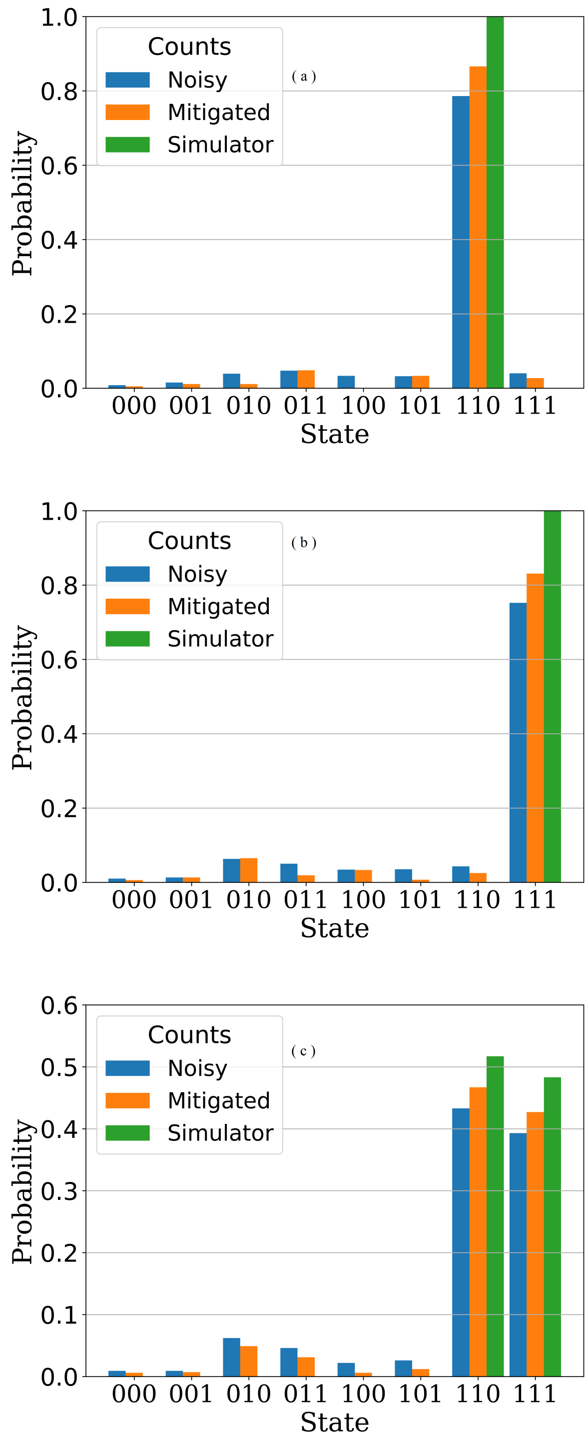

FIGURE 8. Counts for error on third qubit for (a) state $|0\rangle$, (b) state $|1\rangle$ and (c) superposition state.

has lowest error and the state $|1\rangle$ has highest error on the average. The average accuracy of bit flip error correction

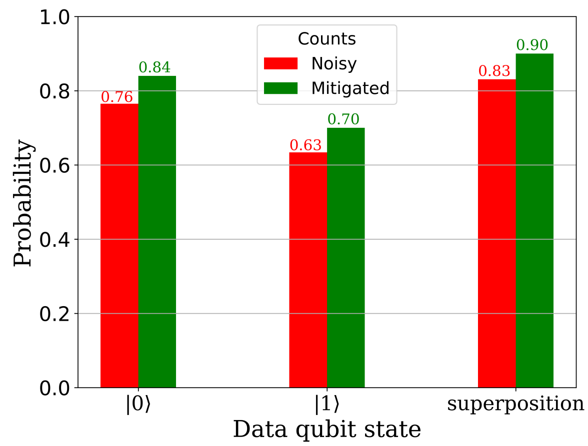

FIGURE 9. Phase-flip error correcting circuit mitigated results.

circuit including error on qubit itself, quantum gates and measurement error is 89.9%$\pm$1.01%. Similarly, for the phase flip error correcting code, the error is high for the state $|0\rangle$ and almost same for other two states. On average phase flip error correction accuracy is found to be 88.05%$\pm$1.89% In this case with the maximum accuracy 90.5%$\pm$1.66% and minimum accuracy 79.7% $\pm$ 5.00%. In addition, for very few number of quantum gates, an error on the individual qubit is same except very small random error and is tested using a simple measurement error mitigation technique. This technique improved our result for bit flip error correction and phase flip error correction code as well. The obtained results show that the error decreases by an average factor of 5.01 % in bit flip error correction and 7.01% in phase flip error correction. These quantum computer of early phase are found to be suitable only for very small and simple quantum experiment. To achieve scalacable quantum computer, noise on qubits and gates should be reduced significantly.

REFERENCES

1. R. P. Feynman, Int. J. Theor. Phys. **21**, 467 (1982).
2. M. A. Nielsen and I. Chuang, "Quantum computation and quantum information," (2002).
3. B. Schumacher, Phys. Rev. A **51**, 2738 (1995).
4. W. G. Unruh, Phys. Rev. A **51**, 992 (1995).
5. P. W. Shor, Phys. Rev. A **52**, R2493 (1995).
6. A. O. Pittenger, *An introduction to quantum computing algorithms*, Vol. 19 (Springer Science & Business Media, 2012).
7. E. Knill and R. Laflamme, Phys. Rev. A **55**, 900 (1997).
8. A. M. Steane, Phys. Rev. A **54**, 4741 (1996).
9. D. Touchette, H. Ali, and M. Hilke, arXiv preprint arXiv:1010.3242 (2010).
10. D. Leung, L. Vandersypen, X. Zhou, M. Sherwood, C. Yannoni, M. Kubinec, and I. Chuang, Phys. Rev. A **60**, 1924 (1999).
11. C. Ottaviani and D. Vitali, Phys. Rev. A **82**, 012319 (2010).

12. E. Knill, R. Laflamme, R. Martinez, and C. Negrevergne, Phys. Rev. Lett. **86**, 5811 (2001).
13. J. Chiaverini, D. Leibfried, T. Schaetz, M. D. Barrett, R. Blakestad, J. Britton, W. M. Itano, J. D. Jost, E. Knill, C. Langer, *et al.*, Nature **432**, 602–605 (2004).
14. C.-K. Li, M. Nakahara, Y.-T. Poon, N.-S. Sze, and H. Tomita, Phys. Lett. A **375**, 3255–3258 (2011).
15. R. Harper and S. T. Flammia, Phys. Rev. Lett. **122**, 080504 (2019).
16. S. B. Bravyi and A. Y. Kitaev, “Quantum codes on a lattice with boundary,” arXiv preprint quant-ph/9811052 (1998).
17. R. Barends, J. Kelly, A. Megrant, A. Veitia, D. Sank, E. Jeffrey, T. C. White, J. Mutus, A. G. Fowler, B. Campbell, *et al.*, “Superconducting quantum circuits at the surface code threshold for fault tolerance,” Nature **508**, 500–503 (2014).
18. C. Ballance, T. Harty, N. Linke, M. Sepiol, and D. Lucas, “High-fidelity quantum logic gates using trapped-ion hyperfine qubits,” Physical review letters **117**, 060504 (2016).
19. X. Rong, J. Geng, F. Shi, Y. Liu, K. Xu, W. Ma, F. Kong, Z. Jiang, Y. Wu, and J. Du, “Experimental fault-tolerant universal quantum gates with solid-state spins under ambient conditions,” Nature communications **6**, 1–7 (2015).
20. A. Noiri, K. Takeda, T. Nakajima, T. Kobayashi, A. Sammak, G. Scappucci, and S. Tarucha, “Fast universal quantum gate above the fault-tolerance threshold in silicon,” Nature **601**, 338–342 (2022).
21. U. Alvarez-Rodriguez, M. Sanz, L. Lamata, and E. Solano, “Quantum artificial life in an ibm quantum computer,” Scientific reports **8**, 1–9 (2018).
22. B. K. Behera, T. Reza, A. Gupta, and P. K. Panigrahi, “Designing quantum router in ibm quantum computer,” Quantum Information Processing **18**, 1–13 (2019).
23. D. Alsina and J. I. Latorre, “Experimental test of mermin inequalities on a five-qubit quantum computer,” Physical Review A **94**, 012314 (2016).
24. E. Knill, R. Laflamme, A. Ashikhmin, H. Barnum, L. Viola, and W. H. Zurek, arXiv preprint quant-ph/0207170 (2002).
25. A. Asfaw, L. Bello, Y. Ben-Haim, S. Bravyi, L. Capelluto, A. C. Vazquez, J. Ceroni, J. Gambetta, S. Garion, L. Gil, *et al.*, URL: https://qiskit. org/textbook/ch-applications/qaoa. html (Accessed 06/21/2021) (2020).